(12) PARAMETRICAL STATIC STUDY ON GROUP STUDS UNDER BIAXIAL ACTION

Chen Xu[1], Kunitomo Sugiura[2]

[1]Member of JSCE, Dept. of Civil & Earth Resources Eng., Kyoto University
(615-8540, Kyoto, Japan)
E-mail: chen.xu@aw4.ecs.kyoto-u.ac.jp
[2]Member of JSCE, Professor, Dept. of Civil & Earth Resources Eng., Kyoto University
(615-8540, Kyoto, Japan)
E-mail: sugiura.kunitomo.4n@kyoto-u.ac.jp

Group studs are known as shear connectors in steel and concrete composite structures. By now, many composite bridges have been characterized by long lateral cantilevers. The studs are actually under biaxial action consisting of shear force and action in light of lateral bending moment on concrete slab induced by long cantilever and passing by moving loads. Moreover, lateral bending moment can result in the initiation of bending-induced concrete cracks. These two situations can both affect mechanical performance of group studs. Thus, a parametrical FEM analysis was carried out to study the mechanical behavior of group studs with respect to biaxial action and initial bending-induced concrete cracks, in which damage plasticity was introduced to simulate material nonlinear behavior. In the analysis, lateral bending moment determined by maximum crack widths of initial bending-induced concrete cracks including 0.1mm and 0.2mm, shank diameters including 13mm, 16mm, 19mm and 22mm and stud heights including 80mm and 100mm were parameters. It was found that shear stiffness of group studs with large shank diameter would be less affected by biaxial action while bending-induced concrete cracks seemed unfavorable to stud shear stiffness. On the other hand, typical push-out tests on group studs were executed to investigate the reliability of FEM analysis

***Key Words**: group studs, FEM analysis, biaxial action, bending-induced crack, shear stiffness*

1 INTRODUCTION

Steel and concrete composite girders have been widely applied in the structures since 1960s. Shear stud, connecting the concrete slab and steel flange of composite structures, has already been used as shear connectors for over 50years for its economical advantage. Arranging studs in group, referred to as group studs, is known for the constructional efficiency, while its deficiencies are also obvious. Nowadays, many composite bridges are characterized by long lateral cantilevers. The lateral bending moment on concrete slab caused by dead loads of cantilevers and passing by vehicle loads may become influential to mechanical status of group studs. Combined with longitudinal interlayer shear forces, the load action imposed on group studs becomes biaxial action. Moreover, initial bending-induced concrete cracks resulted by lateral bending moment may also affect the mechanical performance of group studs. So far, the mechanical behavior of shear stud has been concerned by a large number of researches [1-9]. Generally speaking, they can be categorized into the aspects of the fatigue behavior and the static behavior. However, literatures concerning the shear studs under biaxial action seem rare. Thus a parametrical FEM analysis was accordingly carried out. In this analysis, lateral bending moment, shank diameter and stud height were set as parameters. Since stress concentrations on concrete and stud both initiate at very early load stage near the stud root position as reflected in many push out tests, the damage plasticity model, by defining a damage factor of elastic modulus, was used to reflect the material softening stage. This material damage plasticity model is supported in the general FEM software ABAQUS. For the analysis reliability verification, a typical push out experiment was introduced.

2 NUMERICAL MODEL SETUP

(1) FEM model design

Concerning the mechanical performance of group studs with respect to biaxial action and initial bending-induced concrete cracks, lateral bending moment was considered a parameter. Shank diameter and stud height were also involved. The imposed external loads consisted of a vertical push load and symmetrically distributed lateral loads for activating lateral bending moments as shown in Fig. 1. The loads combination depended on analysis cases including (Ⅰ) uniaxial action, (Ⅱ) biaxial action and (Ⅲ) initial bending-induced concrete cracks and varied with load steps. They are listed in Table 1. Different vertical loading rates have been tried and the optimum rate was found out to be 0.2mm/s.

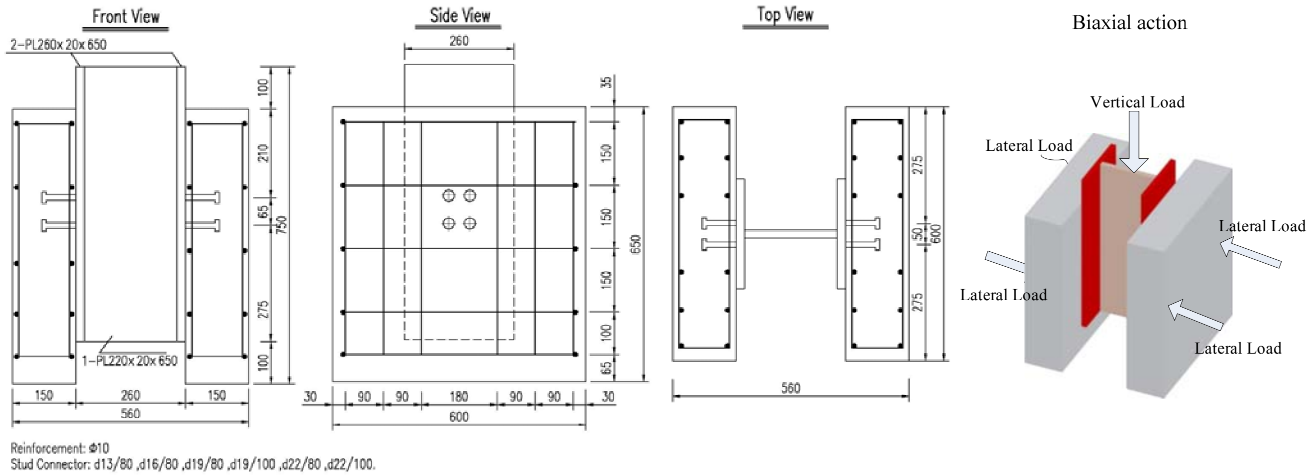

Fig. 1 Layout of FEM model for parametrical study

Table 1 Load combinations in the analysis

Load step	Case Ⅰ	Case Ⅱ		Case Ⅲ	
	Vertical load	Vertical load	Lateral loads	Vertical load	Lateral loads
1	Activate	-	Activate	-	Activate and Deactivate
2	Propagate	Activate	Propagate	Activate	-

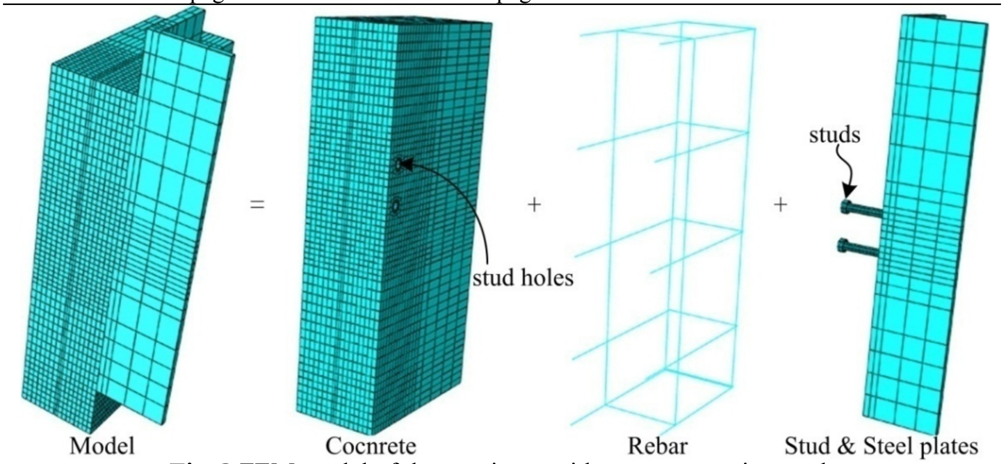

Fig. 2 FEM model of the specimen with group arranging studs

Fig. 2 shows the dimension of FEM models for parametrical study, which was based Eurocode 4[10]. 4 studs were connected to each steel flange, equaling to those of standard push out specimen. The vertical and lateral spacing of studs were respectively 65mm and 50mm in terms of Eurocode 4 [10]. Compared to related specifications in AASHTO [11] and JSCE [12], the minimum spacing values of studs in both directions specified in Eurocode4 are smallest.

In light of geometrical, boundary and loading symmetry in push out specimen, a quarter part of specimen was simulated. Studs and steel component were created in the same part while concrete slab and reinforcements were created in different parts. All parts were assembled together to form the simulation model as shown in Fig. 2. In the model, three dimensional eight nodes reduced integration element (C3D8R) was used to simulate concrete, studs and steel plates while two nodes three dimensional truss element (T3D2) was introduced to simulate embedded reinforcements.

Table 2 Generalization of parametrical models(mm, kN)

Group	Label	Case	L	d	L/d	F_b
A	groupA	I	13	80	6.15	0
	groupABM1	II	13	80	6.15	36
	groupABM2	II	13	80	6.15	76
	groupACM1	III	13	80	6.15	36
	groupACM2	III	13	80	6.15	76
B	groupB	I	16	80	5.00	0
	groupBBM1	II	16	80	5.00	36
	groupBBM2	II	16	80	5.00	76
	groupBCM1	III	16	80	5.00	36
	groupBCM2	III	16	80	5.00	76
C	groupC	I	19	80	4.21	0
	groupCBM1	II	19	80	4.21	36
	groupCBM2	II	19	80	4.21	76
	groupCCM1	III	19	80	4.21	36
	groupCCM2	III	19	80	4.21	76
D	groupD	I	19	100	5.26	0
	groupDBM1	II	19	100	5.26	36
	groupDBM2	II	19	100	5.26	76
	groupDCM1	III	19	100	5.26	36
	groupDCM2	III	19	100	5.26	76
E	groupE	I	22	80	3.64	0
	groupEBM1	II	22	80	3.64	36
	groupEBM2	II	22	80	3.64	76
	groupECM1	III	22	80	3.64	36
	groupECM2	III	22	80	3.64	76
F	groupF	I	22	100	4.55	0
	groupFBM1	II	22	100	4.55	36
	groupFBM2	II	22	100	4.55	76
	groupFCM1	III	22	100	4.55	36
	groupFCM2	III	22	100	4.55	76

Labels and parametrical values of FEM models are generalized in Table 2 where d is shank diameter; L is stud height; F_b is lateral load value. Ⅰ is uniaxial action; Ⅱ is biaxial action; Ⅲ is initial bending-induced concrete cracks. These parametrical FEM models were categorized into 6 groups in light of shank diameter and stud height. The shank diameters included 13mm, 16mm, 19mm and 22mm. And stud height included 80mm and 100mm. As to lateral load, it was determined by bending-induced maximum crack width on concrete slab. Specifically, lateral loads respectively inducing maximum crack widths of 0.1mm and 0.2mm were separately applied. The maximum crack width calculation was given as Eq. (1) based on Ref. [13].

$$\omega_R = C_1 C_2 C_3 \frac{\sigma_{ss}}{E_s}\left(\frac{30+d}{0.28+10\rho}\right) \tag{1}$$

Where ω_R is the maximum crack width; C_1 is the reinforcement surface shape coefficient, $C_1 = 1.0$, C_2 the load effect coefficient, $C_2 = 1.0$, C_3 the mechanical behavior coefficient, $C_2 = 1.15$ for slab under bending moment; σ_{ss} is the reinforcement stress; d is the diameter of reinforcement; ρ is the tensile reinforcement ratio. Accordingly, the corresponding forces were 36kN and 76kN.

(2) FEM material constitutions

As to material constitutions, the uniaxial concrete stress-strain (σ - ε) relationship, as illustrated in Fig. 3, was essentially expressed as Eq. (2) and (3)[14].

$$\sigma = \begin{cases} f_c\left[\alpha_a(\varepsilon/\varepsilon_c)+(3-2\alpha_a)(\varepsilon/\varepsilon_c)^2+(\alpha_a-2)(\varepsilon/\varepsilon_c)^3\right] & , \ \varepsilon/\varepsilon_c \le 1 \\ (f_c\varepsilon/\varepsilon_c)/\left[\alpha_d(\varepsilon/\varepsilon_c-1)^2+\varepsilon/\varepsilon_c\right] & , \ \varepsilon/\varepsilon_c > 1 \end{cases} \tag{2}$$

$$\sigma = \begin{cases} f_t\left[1.2(\varepsilon/\varepsilon_t)-0.2(\varepsilon/\varepsilon_t)^6\right] & , \ \varepsilon/\varepsilon_t \le 1 \\ f_t\,\varepsilon/\varepsilon_t\left[\alpha_t(\varepsilon/\varepsilon_t)^{1.7}+\varepsilon/\varepsilon_t\right] & , \ \varepsilon/\varepsilon_t > 1 \end{cases} \tag{3}$$

Where f_c and f_t are the uniaxial compressive and tensile strength of concrete; ε_c and ε_t are the strains related to compressive and tensile peak stresses; α_a, α_d and α_t are regression parameters. In the analysis, $f_c = 50MPa$, $f_t = 3.0MPa$, $\varepsilon_c = 1920\mu\varepsilon$, $\varepsilon_t = 118\mu\varepsilon$, $\alpha_a = 2.00$, $\alpha_d = 1.00$ and $\alpha_t = 2.81$.

The stress strain relationships of studs, steel plates and reinforcement included elastic and linear hardening stages. In addition, descending stages were also taken account in the materials of stud and reinforcement. The uniaxial stress plastic strain relationships of these materials are illustrated in Fig. 4.

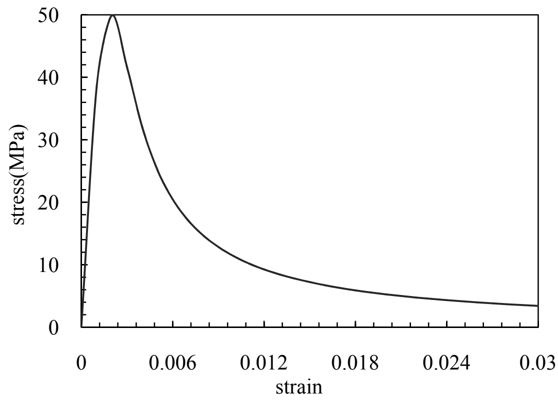

(a) Compression

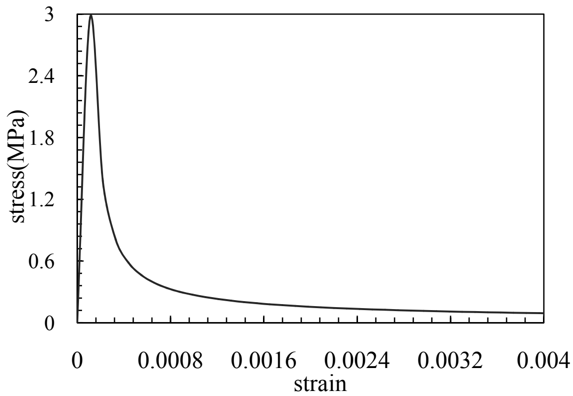

(b) Tension

Fig. 3 Uniaxial concrete stress vs. strain relationships

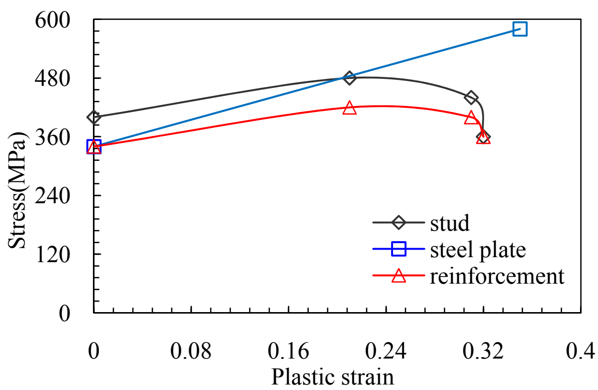

Fig. 4 Uniaxial stress vs. plastic strain relationships of non-concrete materials

Based on the uniaxial material constitutions, damage plastic models were introduced to simulate material nonlinear behaviors of concrete and stud. By defining damage variable D, plastic development can be described as process of modulus degradation.

Concerning concrete compressive damage process, it was assumed that damage initiated when stress just went beyond the peak, 50MPa as shown in Fig. 3(a). The damage evolution can be specified by damage variable D as given in Eq. (4) where E_0 is the initial elastic modulus and E_D is the degraded modulus defined as secant slope of unloading stress-strain curve.

$$D = 1 - E_0 / E_D \tag{4}$$

The unloading stress-strain relationship is expressed as Eq. (5) [15] where σ_1 and ε_1 are the initial stress and strain when unloading process starts. In terms of Eq. (4), the residual strain equals to the product of 0.2 times the initial strain when stress reduces to zero. As long as residual strain is known, E_D can be accordingly calculated.

$$\sigma = \frac{(\varepsilon - 0.2\varepsilon_1)\sigma_1}{1.8\varepsilon_1 - \varepsilon} \tag{5}$$

The concrete tensile damage was assumed to initiate at tensile peak stress, 3MPa as shown in Fig. 3(b). The damage evolution process also follows the same way as specified in concrete compressive damage model.

The uniaxial concrete damage evolution for compressive and tensile are respectively showed in Fig. 5.

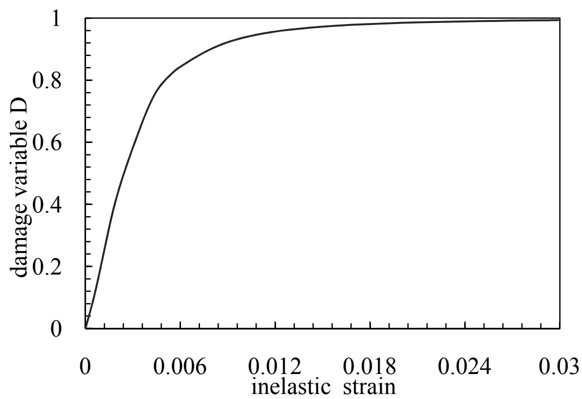

(a) Compression

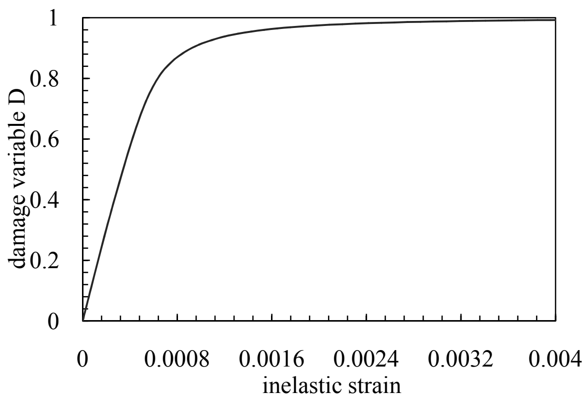

(b) Tension

Fig. 5 Uniaxal concrete damage models

As to damage model of stud, the metal facture strain is actually decided by a couple of factors including strain rate, thermal effect, stress triaxiality, etc. Since the loading rate of 0.2mm/s was considered slow enough to ignore the influence of strain rate and thermal effect, stress triaxiality was viewed as the primary factor. The relationship between stress triaxiality σ_m/σ_{eq} and equivalent fracture strain P_R is expressed as given in Eq. (6)[16], where ε_R refers to the fracture strain under uniaxial load; σ_m is the mean stress; σ_{eq} is the equivalent Mises stress; S_0 is a material constant with the same magnitude of 1, $S_0 = 1.5$, and ν is the possion ratio.

$$P_R = \varepsilon_R \left[\frac{2}{3}(1+\upsilon) + 3(1-2\upsilon)\left(\frac{\sigma_m}{\sigma_{eq}}\right)^2 \right]^{S_0} \tag{6}$$

Moreover, it was assumed that the ratio of P_R to ε_R can approximately equal to the ratio of P_D to ε_D, where ε_D stands for uniaxial strain related to the onset of fracture, and P_D equals to the spatial stress status of fracture initiation. In this sense, the relationship between P_D and ε_D based on P_R and ε_R can be established. It was considered the criteria of fracture initiation as displayed in Fig. 6. For damage evolution, an exponential correlation between damage variable D and plastic displacement has been established based on Ref. [17]. The exponential law parameter was 0.01 and the equivalent plastic displacement was related to dimension size of discrete elements.

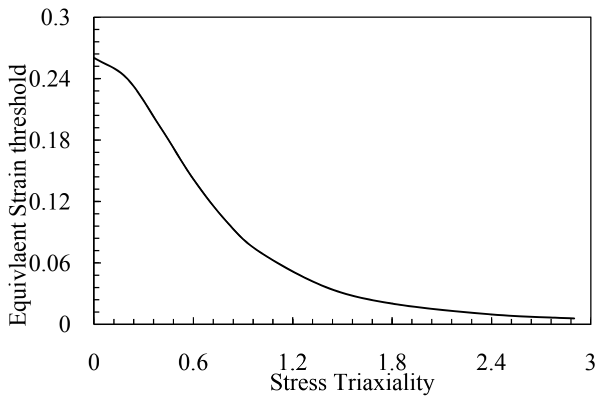

Fig. 6 Criteria of damage initiation on stud

3 NUMERICAL ANALYSIS

Fig. 7 illustrates load-interlayer slip relationships of every push out FEM model listed in Table 2. Among the mentioned three analysis cases, stud shear stiffness of group studs under biaxial action appeared strongest and initial bending-induced concrete cracks resulted in lowest stud shear stiffness. On the other hand, compared to the effect of stud shank diameter on stud shear stiffness, the effect of stud height seemed less significant

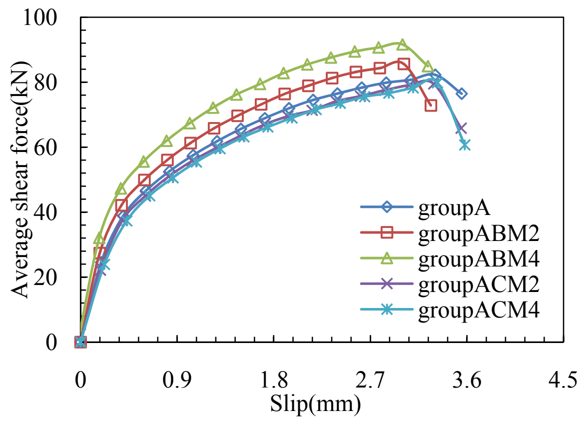

(a) Analyzed load-slip curves of Group A

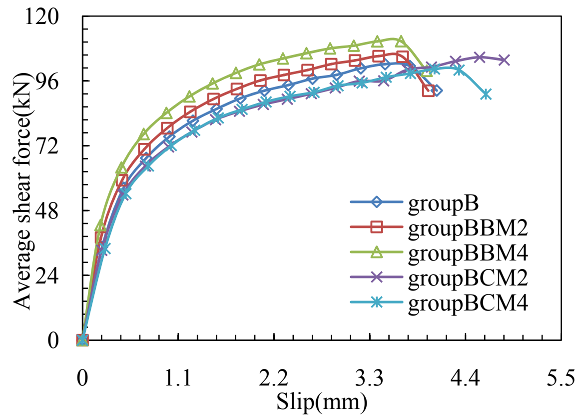

(b) Analyzed load-slip curves of Group B

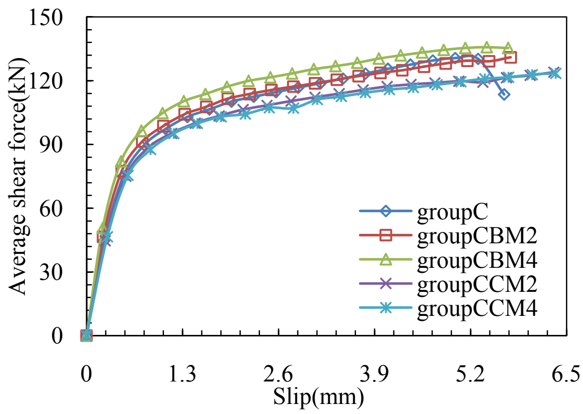

(c) Analyzed load-slip curves of Group C

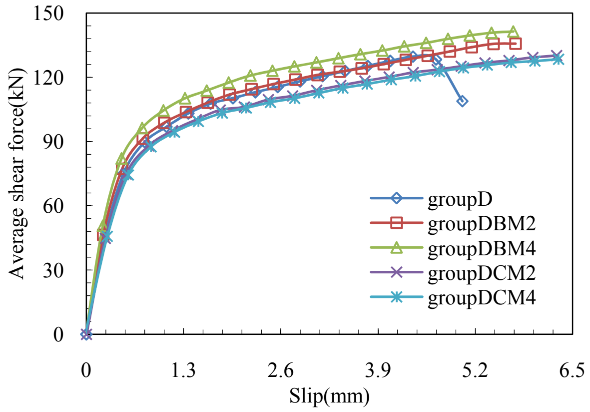

(d) Analyzed load-slip curves of Group D

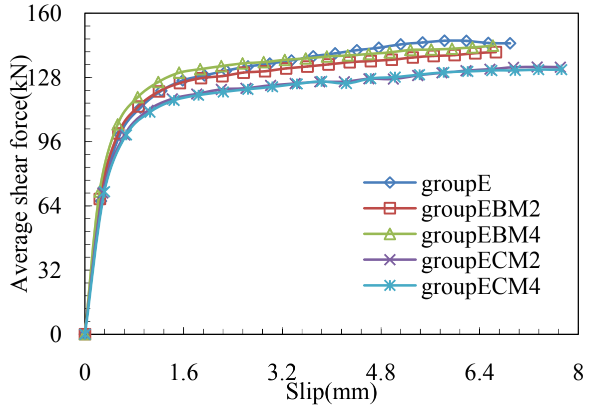

(e) Analyzed load-slip curves of Group E

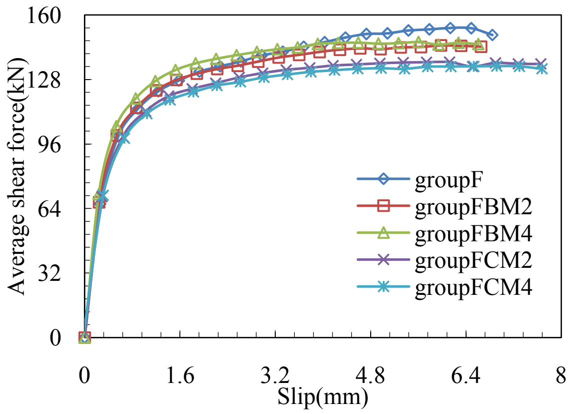

(f) Analyzed load-slip curves of Group F

Fig. 7 Parametrical analyzed load-slip curves

Regarding the influence of biaxial action on stud shear stiffness of group studs, as listed in Table 3 including related results of analysis case Ⅰ and Ⅱ and comparison, it reveals stud shear stiffness increased because of biaxial action. In table 3, d is shank diameter; L is stud height; F_b is lateral load value; K is average shear stiffness of one stud; σ_b is lateral compressive stress value; σ_u is uniaxial compressive strength, σ_u=50MPa. The numeral subscripts stand for the types of biaxial action. Actually, the concrete near stud root performed plastically in a fairy early stage of loading process, at which interlayer slip was still increasing linearly with shear force. This plastic performance, properly as a result of stress concentration, would definitely affect stud shear stiffness. In detail, when biaxial action was activated, the concrete underneath stud root in the direction of interlayer faces was in biaxial compressive status and thus its strength was improved. In this sense, the increase of stud shear stiffness under biaxial action is reasonable. It was also confirmed by that stud shear stiffness increment of each parametrical group exhibits a direct proportion with the ratio of lateral compressive stress σ_b to uniaxial compressive strength σ_u. However, the increase percentage of stud shear stiffness reflected an inverse proportion with shank diameter. This proportional relationship at least indicates that shear stiffness of stud with small shank diameter is more likely affected by non-uniaxial loading action thus application of stud with large shank diameter should be a favorable choice for its stable mechanical performance.

Table 3 Analyzed shear stiffness and increment of case Ⅰ and Ⅱ

Group	d×L (mm^2)	Biaxial Action(kN/mm,MPa)					Increament			
		F_{b0}=0kN	F_{b1}=36kN		F_{b2}=76kN		F_{b1}=36kN		F_{b2}=76kN	
		K_0	K_1	σ_{b1}	K_2	σ_{b2}	K_1/K_0	σ_{b1}/σ_u	K_2/K_0	σ_{b1}/σ_u
A	13×80	128.1	147.0	4.61	175.1	12.10	1.15	0.09	1.37	0.24
B	16×80	158.0	179.7	4.48	205.6	10.51	1.14	0.09	1.30	0.21
C	19×80	185.5	211.2	4.40	234.8	11.38	1.14	0.09	1.27	0.23
D	19×100	184.1	209.4	4.48	235.3	11.33	1.14	0.09	1.28	0.23
E	22×80	269.9	291.9	3.88	313.4	8.16	1.08	0.08	1.16	0.16
F	22×100	269.7	289.3	3.32	311.2	8.00	1.07	0.07	1.15	0.16

Table 4 includes results of analysis cases Ⅰ and Ⅲ and comparison. It shows initial bending-induced concrete cracks caused a reduction of stud shear stiffness. Although rigid conclusion about the relationship between shank diameter and shear stiffness reduction cannot be derived based on the present analysis results, it indicates a tendency that shear stiffness of stud with large shank diameter was less affected. Quantitatively, when initial bending-induced concrete cracks was resulted by lateral load of 36kN, equivalent to the maximum crack width 0.1mm based on Eq. (1), shear stiffness was reduced by 5% at most. This reduction percentage increased to 15% when lateral load became 36kN which could initiate a 0.2mm maximum crack width based on Eq. (1).

Table 4 Shear stiffness of case Ⅰ and Ⅲ (kN/mm)

Group	d×L	F_{b0}=0	F_{b1}=36		F_{b2}=76	
		K_0	K_1	K_1/K_0	K_2	K_2/K_0
A	13×80	128.1	121.2	0.95	98.7	0.77
B	16×80	158.0	155.5	0.98	133.2	0.84
C	19×80	185.5	177.7	0.96	164.6	0.89
D	19×100	184.1	176.0	0.96	163.5	0.89
E	22×80	269.9	262.1	0.97	235.3	0.87
F	22×100	269.7	261.6	0.97	233.1	0.86

4 ANALYSIS RELIABILITY

In order to warrant the reliability of the FEM analysis, in which damage plasticity models were introduced, a verification study, concerning a push out static test on group studs, was executed. As shown in Fig. 8, 9 studs were welded to each steel flange of the test specimens labeled with QT1, QT2 and QT3. The longitudinal and lateral spacing of studs were 60mm and 50mm. The displayed post pour pocket on the concrete slab was filled by high strength mortar. The tested compressive strength of concrete and mortar were 74.3MPa and 75.5MPa, respectively. In light of symmetry, a quarter of the specimen was simulated in the FEM analysis, as shown in Fig. 8. It consisted of solid elements, shell elements and rebar elements. The load was vertically exerted in the form of displacement.

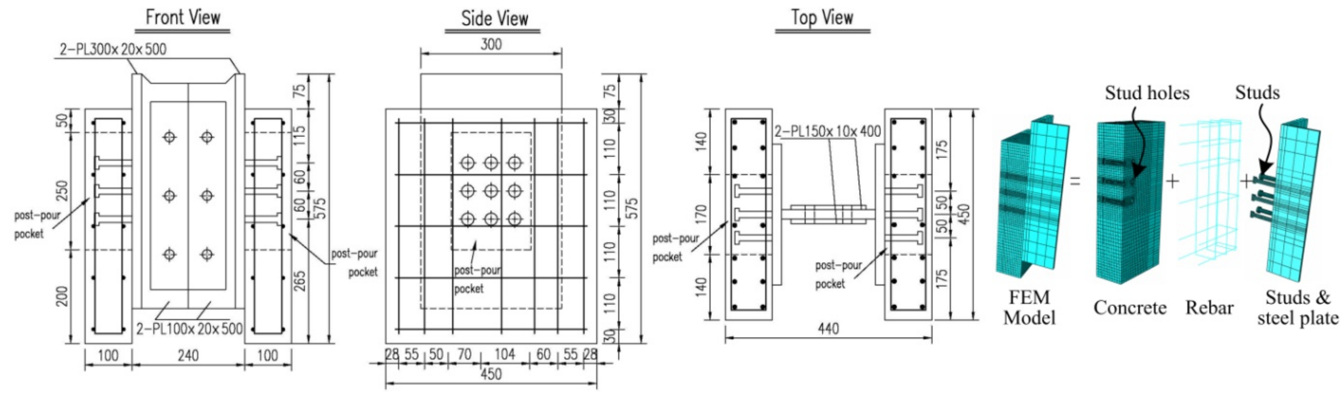

Fig. 8 Layout of push out specimen and related FEM model

In the FEM verification, the material constitution took the real tested data derived from the push out test. And the damage plasticity model was according established.

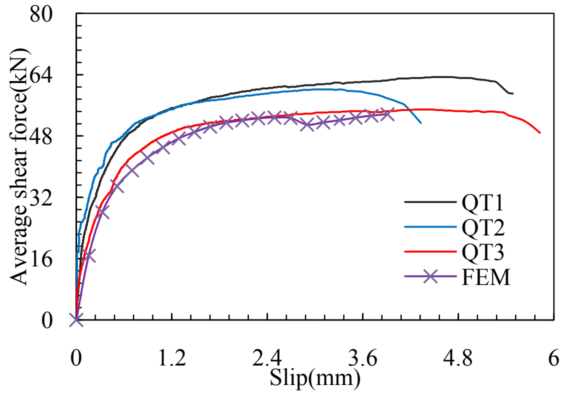

Fig. 9 Load-slip curves of test and FEM analysis

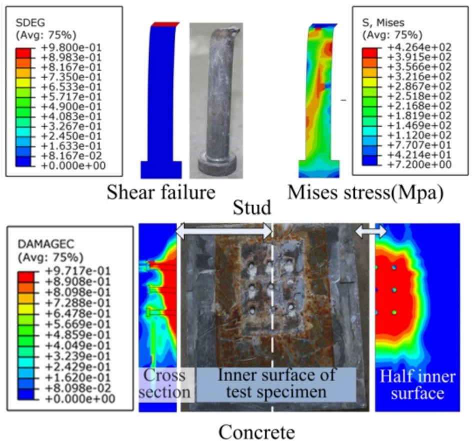

Fig. 10 Failure mode of test and FEM analysis

Fig. 9 shows the comparison between test and FEM analysis on load-slip curve. It shows good coincidence. The down half of Fig. 10 displays concrete damage areas found in the test specimen and that evaluated by FEM analysis. The compressive damage area on the inner side surface derived from the analysis was close to the test result. The up half of Fig. 10 exhibits the experimental failure mode, numerical failure mode and the numerical Mises stress distribution at failure stage of stud. It reveals that shear failure was dominant in either of the experiment and the numerical analysis while bending effect was not significant but indeed existed. The Mises stress distribution shows that the location with maximum Mises stress value had already moved away from the stud root, implying the occurrence of the unloading process near the stud root because of the shear failure. Based on the comparisons, it is convincing to say that the FEM analysis, introducing plasticity damage model, is reliable basically.

5 CONCLUSION

The mechanical behavior of group studs under biaxial action was concerned by nonlinear parametrical FEM analysis. And the reliability of this FEM analysis in was also confirmed based on a typical push out experiment. The following conclusions may be drawn from the present study:

1. According to analysis results, the biaxial action which introduced the biaxial compressive status to concrete seemed favorable for increasing the shear stiffness of studs. Moreover, this effect appears less significant when the shank diameter becomes larger.
2. According to analysis results, the initial cracks on concrete slab results in the reduction of shear stiffness.
3. The damage plasticity models were introduced to simulate the material constitutions of concrete and stud in the FEM analysis. By comparing the analysis results with the test results, the FEM analysis was verified.

ACKNOWLEDGMENT: The push out test in this research is sponsored by National Key Technology R&D Program of China (Grant No. 2007AA11Z105) and Shanghai Urban Construction & Communications Great Research Program (2007-21), China. These supports are gratefully acknowledged.

REFERENCE

1) D.J.Oehlers, C.G.Coughlan. The shear stiffness of stud shear connections in composite beams. Journal of constructional steel research; v6 1986: 273-284.
2) R.P.Johnson. Resistance of stud shear connectors to fatigue. Journal of constructional steel research. 56(2000):101-116.
3) Gerhard Hanswille, Markus Porsch, Cenk Ustundag. Resistance of headed studs subjected to fatigue loading, Part 1: experimental study. Journal of constructional steel research. 63(2007):475-484.
4) Gerhard Hanswille, Markus Porsch, Cenk Ustundag. Resistance of headed studs subjected to fatigue loading, Part 2: analytical study. Journal of constructional steel research. 63(2007):485-493.
5) Chang-Su Shim, Pil-Goo Lee, Tae-Yang Yoon. Static behavior of large stud shear connectors. Engineering structures. 26(2004):1853-1860.
6) Jun Okada, Teruhiko Yoda, Jean-Paul Lebet. A study of the grouped arrangements of stud connectors on shear strength behavior. Structural engineering/Earthquake engineering, JSCE 2006.4; Vol.23, No.1: 75-89.
7) Pil-Goo Lee, Chang-Su Shim, Sung-Pil Chang. Static and fatigue behavior of large stud shear connectors for steel-concrete composite bridges. Journal of constructional steel research. 61(2005):1270-1285.
8) Shiming Chen, Xindi Wang, Yuanlin Jia. A comparative study of continuous steel-concrete composite beams prestressed with external tendons: experimental investigation. Journal of constructional steel research 2009;65:1480-1489.
9) R.Seracino, D.J. Oehlers, M.F.Yeo. Behavior of stud shear connectors subjected to bi-directional cyclic loading. Advances in structural engineering. 2003,v6, No.2.
10) EUROCODE 4. EN 1994. Design of composite steel and concrete structures. Part 2 General rules and rules for bridges.2005
11) AASHTO. LFRD bridge design specifications, 4th edition, American Association of State Highway and Transportation Officials. 2007
12) Committee of steel structure: Standard specification for steel and composite structures (Design edition). JSCE.

2007. [in Japanese].

13) Code for design of concrete structures, GB50010-2002. Ministry of housing and urban-rural development of China, 2002. [in Chinese].

14) Code for design of concrete structures, GB50010-2002. Ministry of housing and urban-rural development of China, 2002. [in Chinese].

15) Zhu Bolong, Dong Zhenxiang. Nonlinear study on reinforced concrete. 1st ed, Shanghai: Tongji University Press; 1985.[in Chinese]

16) Jean Lemaitre. A continuous Damage Mechanics model for ductile fracture. Journal of engineering materials and technology. 1985.1,v107/83.

17) ABAQUS Documentation, version 6.8.1